Experimental Studies on Dust Formation in Space

Shogo Tachibana[1]

Department of Natural History Sciences, Hokkaido University
N10W8 Sapporo, Hokkaido 060-0810, Japan
E-mail: `tachi@ep.sci.hokudai.ac.jp`

Aki Takigawa

Department of Geology. & Mineralogy, Kyoto University
Kitashirakawaoiwake-cho, Kyoto 606-8502, Japan
E-mail: `takigawa@kueps.kyoto-u.ac.jp`

Equilibrium condensation calculations provide a set of stable minerals under a certain physical and chemical condition, but condensation does not necessarily occur in equilibrium in time-variant circumstellar systems, where pressure, temperature, and gas chemistry vary with time. It is of much importance to understand the kinetic aspect of dust formation processes, especially the vapor growth kinetics of dust (condensation and evaporation coefficients, α_c and α_e, representing kinetic hindrances for surface atomistic processes). In this paper, we review condensation and evaporation experiments on metallic iron and forsterite (Mg_2SiO_4), both of which are major dust-candidate minerals; (1) condensation and evaporation of metallic iron proceed without significant kinetic hindrances ($\alpha_c \approx \alpha_e \approx 1$), (2) evaporation of forsterite occurs less effectively than that predicted by the kinetic theory of gasses (α_e=0.1–0.02), (3) evaporation of forsterite is anisotropic, which leads to a specific shape of forsterite dust with a specific relationship to a crystallographic orientation, which is called as a "crystallographically anisotropic shape", and (4) the crystallographically anisotropic shape of anisotropic dust is a potentially powerful probe to evaluate circumstellar dust-formation processes and conditions. We also show our recent progresses in condensation experiments on forsterite under protoplanetary disk conditions, where polycrystalline forsterite was obtained as condensates under controlled pressure and temperature conditions (hydrogen pressure of 5.6 Pa and temperature of 1275 and 1160 K). Preliminary results indicate that the condensation coefficient of forsterite (α_c) is smaller than unity (α_c=0.09–0.006) and is consistent with α_e. The smaller α_c of forsterite than that of metallic iron implies that forsterite dust forms less efficiently than metallic iron in circumstellar environments.

1

Speaker

1.Introduction

Thermodynamics tells us what kinds of minerals are stable under various chemical conditions in space [e.g., 1]. In the system of solar composition, refractory minerals enriched in calcium and aluminum, such as corundum (Al_2O_3), hibonite ($CaAl_{12}O_{19}$), spinel ($MgAl_2O_4$), and melilite ($Ca_2Al_2SiO_7$-$Ca_2MgSi_2O_7$), are the stable phases at high temperatures. Forsterite (Mg_2SiO_4), enstatite ($MgSiO_3$), and metallic iron become stable at lower temperatures.

These minerals have been found in chondrites, primitive groups of meteorites, indicating that dust formation occurred in the early stage of the solar-system evolution. Calcium, aluminum-rich inclusions (CAIs) consist mainly of refractory minerals that are predicted to condense at high temperatures in thermodynamical calculations, and amoeboid olivine aggregates (AOAs) are fine grained aggregates of forsteritic olivine grains, also suggesting the condensation origin in the solar system [e.g., 2]. Chondrites contain various circumstellar "presolar" grains with anomalous isotopic compositions as well. Presolar grains, including diamond, SiC, corundum, spinel, silicates, graphite, and nano-diamond, are the condensates in circumstellar environments prior to the solar-system formation [e.g., 3, 4].

Thermodynamics, however, does not provide the information on what and how the grain sizes and the number density of condensates were determined and how long the condensation process lasted. Moreover, the presence of components that are stable at various temperatures requires the isolation of condensates from lower temperature reactions, which may be caused by physical separation and/or sluggish chemical reactions. These issues should be discussed with kinetics of dust formation processes [e.g., 5].

There have been many experimental studies on dust formation under non-equilibrium conditions [e.g., 6]. We have been particular about evaporation and condensation experiments of dust-analogue minerals [7, 8] under the conditions as close as possible to real circumstellar conditions such as pressure, temperature, and chemistry because processes that control dust formation could be different under different physicochemical conditions. In this paper, we first review evaporation and condensation experiments for metallic iron [7] and forsterite [8], both of which are major dust forming minerals in space. We also show our recent progress in condensation experiments on forsterite under protoplanetary disk conditions.

2.Condensation of metallic iron

Condensation experiments on metallic iron were carried out in vacuum to determine the condensation kinetics [7]. The concept of condensation experiments of metallic iron is shown in Figure 1. A metallic iron pellet put inside an alumina tube was used as a gas source of iron. The alumina tube guided the evaporated gas to the substrate of alumina disk, which was put in a cooler region of the furnace. The substrate temperatures were 1235 and 1340 K, which are the temperatures close to condensation of metallic iron in protoplanetary disks [1]. The incoming gas flux through the tube reaches the steady state and can be calculated from the kinetic theory

of gases and the weight loss of gas source. The partial pressure of iron gas at the surface of substrate was thus controlled and kept constant during experiments.
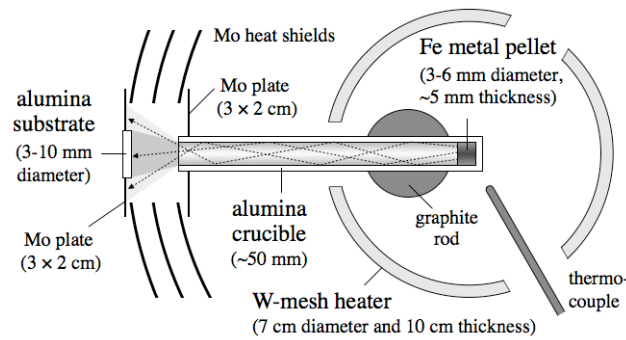

Figure 1: Schematic illustration of experimental setup for condensation of metallic iron (modified from reference [7]).

A compact layer of metallic iron was obtained on the alumina substrate (Figure 2), and both the weight loss of the gas source due to evaporation and the weight gain of the substrate due to condensation varied linearly with time (Figure 3).
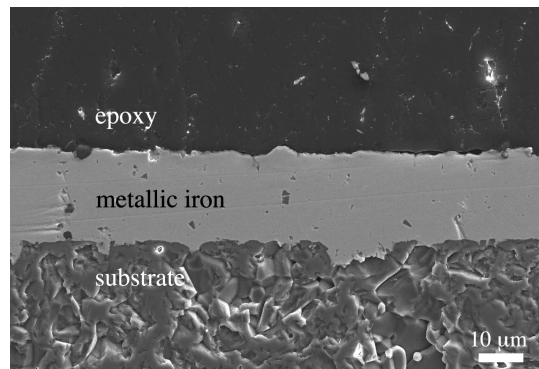

Figure 2: Secondary electron image of the cross section of metallic iron condensed at 1235 K for 48 hours (modified from reference [7]).
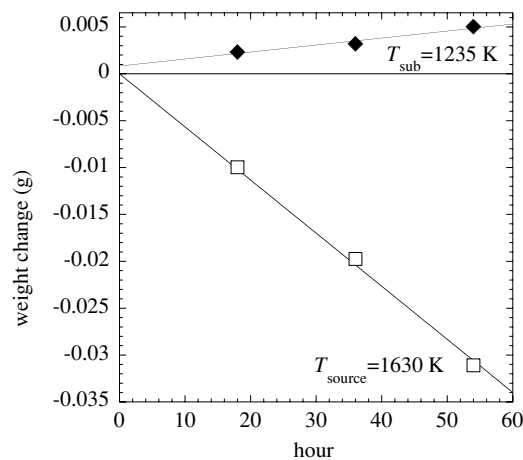

Figure 3: Weight loss of metallic iron (gas source) due to evaporation at 1630 K and weight gain of the substrate (1235 K) due to condensation of metallic iron (from reference [7]).

This linear correlation suggests that the growth rate of metallic iron is controlled by a supply of Fe atoms to the surface sites energetically favorable to crystal growth. The vapor growth rate of metallic iron is expressed with the Hertz-Knudsen equation as a function of the partial pressure of metallic iron (p_{Fe}), the equilibrium vapor pressure of metallic iron (p^{eq}_{Fe}) and temperature (T) [9]:

$$J = \frac{\alpha_c p_{Fe} - \alpha_e p^{eq}_{Fe}}{\sqrt{2\pi M_{Fe} RT}},$$

(2.1)

where M_{Fe} is the molar weight of iron, R is the gas constant, and α_c and α_e are the condensation and evaporation coefficients, respectively, ranging from 0 to 1 to represent kinetic hindrances for surface atomistic reactions. The evaporation coefficient (α_e) of metallic iron in vacuum (p_{Fe}=0) has been known to be close to unity [7].

The condensed fluxes of metallic iron, obtained from weight-gain rates of the substrates at 1235 and 1340 K, are shown as a function of the supersaturation ratio with calculated condensation fluxes with different values of α_c and α_e ($\alpha_c=\alpha_e$ is assumed) in Figure 3. The fluxes are normalized to the ideal evaporation flux that is given by an absolute value of equation 2.1 with p_{Fe}=0 and α_e=1. All the obtained condensation fluxes are close to the ideal maximum condensation flux with $\alpha_c=\alpha_e$=1. This implies that there is little kinetic hindrance for growth of metallic iron and all the atoms colliding the surface condense efficiently. Note that α_c of unity is obtained in this study irrespective of α_e because S is larger than 10 and the effect of α_e is not significantly large compared to the uncertainties in condensed fluxes.

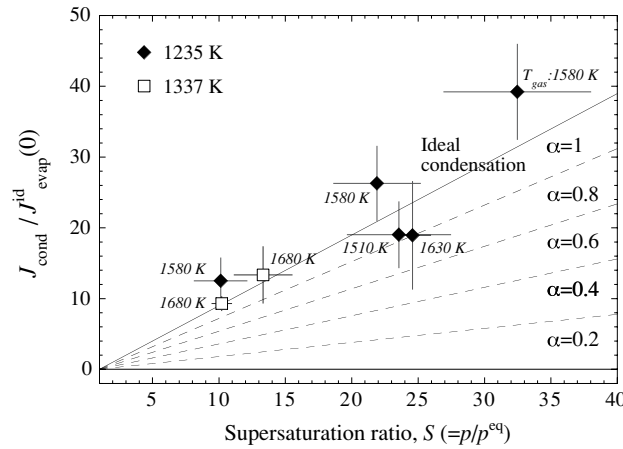**Figure 4:** Condensation flux (J_{cond}) of metallic iron, normalized to the ideal evaporation rate ($J^{id}_{evap}(0)$), plotted against the supersaturation ratio, S (from reference [7]). Solid and open symbols represent the fluxes obtained at the substrate temperatures of 1235 and 1337 K, respectively. Temperatures shown with symbols (T_{gas}) represent temperatures of iron gas. The ideal condensation flux ($\alpha=\alpha_c=\alpha_e$=1) is shown as a solid line, and the fluxes with different values of α_c are also shown (dashed lines).

3.Evaporation of forsterite

Evaporation kinetics of forsterite has been intensively studied in vacuum and in low-pressure hydrogen gas at the temperature range of 2073–1153 K [e.g., 8, 10, 11]. Forsterite evaporates congruently and thus its evaporation rate can be expressed by the Hertz-Knudsen

equation. The evaporation coefficients of forsterite obtained in previous studies are smaller than unity and ranges from 0.1-0.02 in wide ranges of temperature and hydrogen pressure (Figure 5). It has been known that evaporation of forsterite proceeds anisotropically in vacuum [10, 11] and in hydrogen gas [8] and that the anisotropy depends on temperature and hydrogen gas pressure (Figure 5).
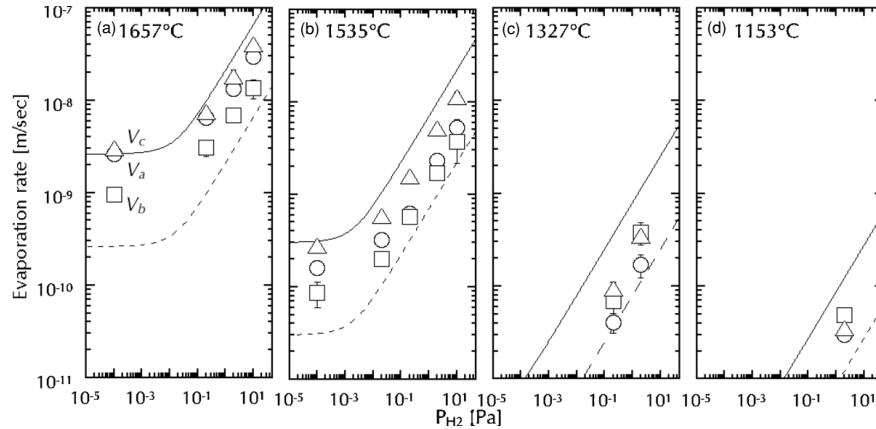
Figure 5: Evaporation rates of forsterite along three crystallographic axes plotted as a function of hydrogen pressure (from reference [8]). Evaporation rates in vacuum are also plotted at 10^{-4} Pa. Open circles, squares, and triangles represent the rates along the a-, b-, and c-axes, respectively. The evaporation rates with α_e of 0.1 and 0.01 are shown as solid and dotted curves for comparison.

Takigawa et al. (2009) [8] suggested that anisotropic evaporation of forsterite leads to a specific shape of forsterite dust with a specific relationship to a crystallographic orientation, which is called as "crystallographically anisotropic shape," depending on the evaporation condition. Takigawa and Tachibana (2012) [12] showed that the change of the crystallographically anisotropic shape of forsterite by evaporation causes observable changes of infrared features (Figure 6), and that the crystallographically anisotropic shape is a potentially powerful probe to evaluate circumstellar dust-forming conditions. They applied their model to the spectrum of a protoplanetary disk HD100546 and found that a certain fraction (~25%) of forsterite dust may have experienced high-temperature evaporation (>1600 K) (Figure 7).
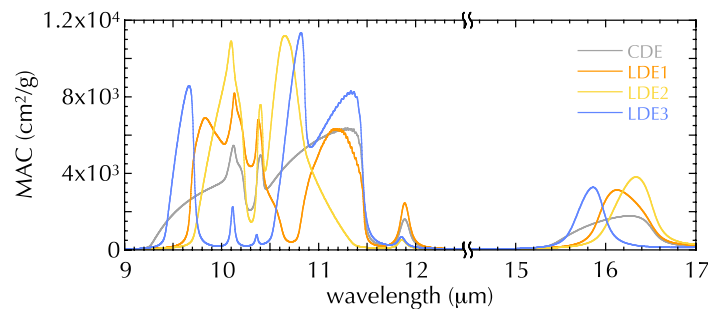
Figure 6: Mass absorption coefficients of forsterite at 100 K with limited distributions of ellipsoids (LDE1, LDE2, and LDE3) with that of CDE (continuous distribution of ellipsoids) (from reference [12]). LDE1 and LDE2 represent ensembles of shapes possibly formed by evaporation at >1600 K and at <1600 K, respectively; Disk-like forsterite grains flattened to the c-axis and disk flattened to the b-axis dominate in LDE1 and LDE2, respectively. Forsterite grains elongated along the c-axis dominate in LDE3.
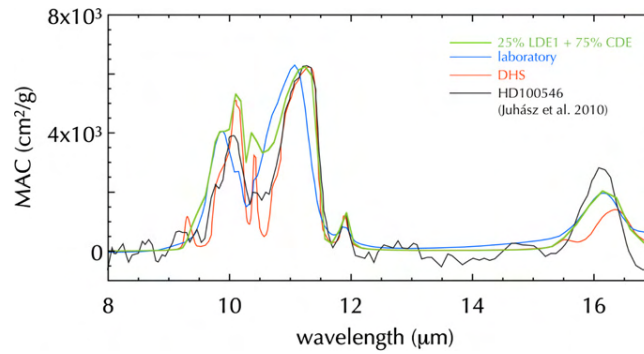
Figure 7: Comparison of the mass absorption coefficient of forsterite as a composite spectrum of 75% of CDE and 25% of LDE1 (100 K) with the spectrum of the protoplanetary disk HD100546 (from reference [12]). The DHS spectrum (distribution of hollow spheres) and the laboratory spectrum of forsterite are also shown. The vertical axis is arbitrary.

4.Condensation of forsterite

Condensation kinetics of forsterite under low-pressure conditions has not yet investigated in detail in spite of its importance. In order to understand condensation kinetics of forsterite, we have carried out condensation experiments under protoplanetary disk-like conditions in the system of Mg_2SiO_4-H_2-H_2O.

4.1Experiments

An infrared vacuum furnace was used in this study, consisting of a silica glass tube (~300 mm in length and 38 mm in diameter) connected to a pumping system and two infrared heating systems. The furnace was continuously evacuated during experiments. A mixed gas of H_2 and H_2O was flowed into the system at a controlled rate to keep a pressure constant. Synthetic forsterite powder in an Ir crucible was heated as a gas source. A part of evaporated gases were condensed on a substrate of Pt mesh located at a cooler region in the chamber (15-25 mm from the gas source). The substrate temperature was monitored by a type-R thermocouple.

The pressure and temperature conditions were close to those of protoplanetary disks. The total pressure of the system was ~5.5 Pa (5.5×10^{-5} bar), and the substrate temperature were 1320, 1275, and 1160 K with ±5-10 K fluctuation. The H_2O/H_2 ratio was set at 0.015, which was ~15 times larger than the solar ratio. The SiO/H_2 ratio was evaluated to be ~0.7-3 % of the solar ratio from the weight loss rate of the gas-source forsterite. Experimental duration ranged from 6 to 237 hours.

Condensates were observed with a field-emission scanning electron microscope (FE-SEM; JEOL JSM 7000F) and their chemical composition and crystallinity were analyzed with energy dispersive X-ray spectroscopy (EDS; Oxford X-Max[N] 150), electron backscattered diffraction (EBSD; HKL CHANNEL 5), and Fourier transform infrared spectroscopy (FTIR; JASCO FT/IR-4200). Transmission electron microscope (TEM; JEM-2100F) observation was also made for focused ion beam (FIB; FEI Quanta 200 3DS) lift-out sections of condensates obtained at 1160 K for 93 hours.

4.2 Condensates

Sub-micron to micron-sized condensates covered with Pt substrates at 1160 and 1275 K (Figure 8), but no condensate was found at 1320 K. The typical size of condensates at 1160 K was sub-micron to 1 μm irrespective of experimental duration and no effective growth of each condensed grain was observed (Figure 8). Condensates at 1275 K for >40 hours partly had several micron-sized flat regions (Figure 8).
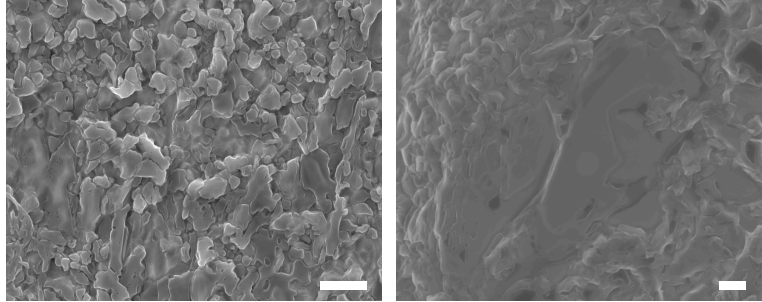

Figure 8: Condensates of forsterite at 1160 K for 93 hours (left) and at 1275 K for 115 hours (right). Scale bars are 1 μm.

Chemical compositions of condensates were consistent with stoichiometric forsterite. A variety of EBSD patterns corresponding to crystalline forsterite were obtained from the condensates. A FIB-section of the condensates at 1160 K showed that condensates were ~30-150 nm in thickness, and their selected area diffraction patterns were indexed to forsterite with different crystallographic orientations. We thus conclude that the condensates are a thin film of polycrystalline forsterite. Infrared absorption spectra of the condensates showed clear 10-μm absorption features, confirming the condensation of crystalline forsterite as well (Figure 9).
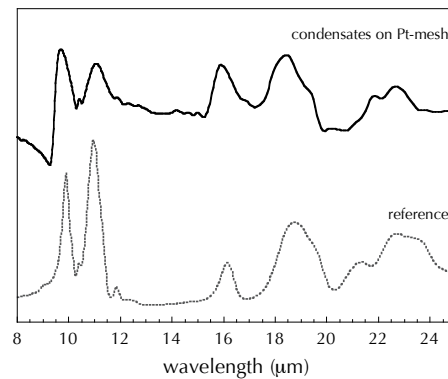

Figure 9: An infrared absorbance of condensates formed at 1275 K for 115 hours (upper spectrum) compared with that of crystalline forsterite (lower spectrum). The vertical unit is arbitrary. The FTIR analysis was made directly for a platinum mesh with condensates without any dispersion into medium.

4.3 Growth process of forsterite

We first discuss the supersaturation conditions in the present study. The mean free path of gas molecules under the present experimental conditions is less than 1 mm, and the

evaporated forsteritic gas and the ambient H_2-H_2O gas are expected to be well mixed.   The supersaturation ratio is defined here as the ratio between the incoming flux of SiO to the surface of the substrate and the ideal evaporation flux of forsterite at the substrate temperature (p_{SiO}=0 and α_e=1 in equation 2.1).   The incoming flux of SiO to the surface of substrate is estimated from the weight loss of the gas source, and the ideal evaporation flux of forsterite is obtained thermodynamically.   The silica glass tube used as a vacuum chamber may have acted as a sink of evaporated gases due to condensation onto the wall, and considering the uncertainty of the amount of condensed gas onto the wall, the supersaturation ratios (S) for experiments at 1320, 1275, and 1160 K are estimated to be 1–5, 7–190, and 800–8000.   These supersaturation ratios correspond to the supercooling of 0-50, 40–150 and 160–230 K, respectively.

No condensate was found at 1320 K because the degree of supersaturation was too small for nucleation of forsterite or even the vapor was not saturated with forsterite ($S \approx 1$).   The condensates at S of 800–8000 (1160 K) imply that heterogeneous nucleation of new grains occurred successively on preexisting grains (Figure 8).   On the other hand, at S of 7–190 (1275 K), some grains seem to have grown up to several to ten μm, while some seem to have newly nucleated on preexisting grains (Figure 8).   This suggests that both nucleation and growth of each condensate occurred at S of 7–190.

These differences would result in a structural difference in forsterite dust condensed in protoplanetary disks.   Aggregates of sub-micron sized fine particles would form with a high supersaturation (>1000), while aggregates containing micron-sized grains would form with a supersaturation of <100.   Although further investigation is needed, the formation condition of AOAs in chondrites may be quantitatively found in this experimental setup.

4.4 Growth kinetics of forsterite

The flux condensed on the substrate is expressed by the Hertz-Knudsen equation (equation 2.1).   Figure 10 shows the condensed fluxes of forsterite at different runs under the condition of 1275K and pH$_2$ of 5.6 Pa, which are obtained from weight gains of the substrates.   The estimated incoming fluxes of SiO onto the surface of substrate (vertical solid lines) and an evaporation flux of forsterite at the substrate temperature with α_e of 0.03 (dashed line) [10] are also compared in the Fig. 11.   Based on these fluxes in Figure 10 and equation 2.1, the ranges of α_c are estimated to be 0.006–0.09 (Figure 11).   Although the current estimate of α_c has a relatively large uncertainty due to the uncertainty of S and is needed to be refined in the future study, the α_c at 1275 K is consistent with the evaporation coefficient for forsterite in hydrogen gas [8] and is smaller than that of metallic iron ($\alpha_c \sim \alpha_e \sim 1$).   The difference in α_c and α_e for metallic ion and forsterite may be attributed to the difference in atomic bonds in metallic iron (metallic bonds) and silicates (ionic and/or covalent bonds).   This difference implies that the growth of forsterite dust occurs less efficiently than that of metallic iron dust in circumstellar environments although they have similar equilibrium condensation temperatures.
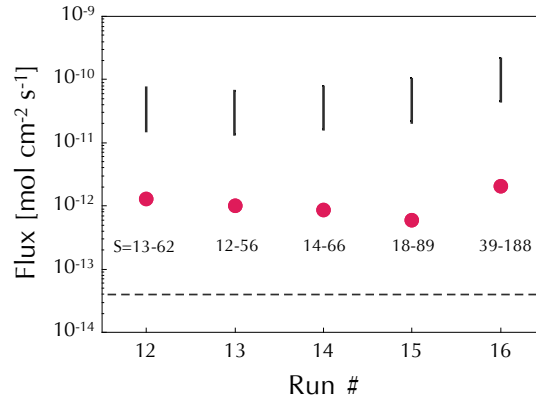
Figure 10: Condensed fluxes of forsterite on Pt-mesh substrates for five runs at 1275K and pH_2 of 5.6 Pa (closed symbols). The ranges of incoming fluxes of SiO onto the surface of substrates evaluated from the weight losses of gas-source forsterite (vertical solid lines) and the expected evaporation flux of forsterite at 1275 K (dashed line) with α_e of 0.03 [8] are also plotted. The ranges of *S* are also shown.
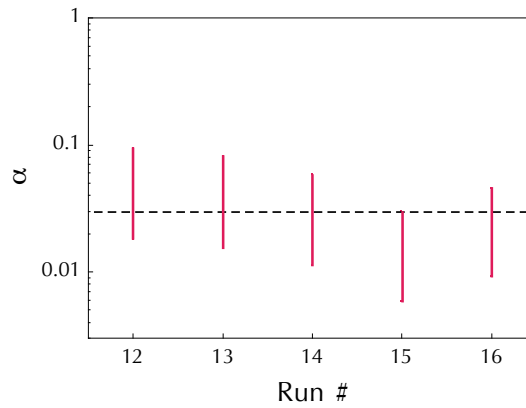

Figure 11: The ranges of α_c evaluated for runs at 1275K and pH_2 of 5.6 Pa. The α_e of 0.03 at 1426 K and pH_2 of 2 Pa is also shown for comparison (dashed horizontal line).

5.Summary

It is important to understand the kinetic aspect of dust formation processes in space, especially the vapor growth kinetics of dust, because dust formation occurs in time-variant circumstellar environments. Condensation and evaporation rates of metallic iron and forsterite, major dust-forming minerals, under low-pressure conditions are expressed by the Hertz-Knudsen equation derived from the kinetic theory of gases. The condensation and evaporation coefficients are dimensionless parameters in the Hertz-Knudsen equation, ranging from 0 to 1, reflect surface kinetic hindrances of condensation and evaporation processes. These kinetic parameters are crucial to understand the formation and evolution of circumstellar dust particles.

Experimental studies have shown that the evaporation and condensation coefficients of metallic iron in vacuum are close to unity, suggesting that evaporation and condensation of metallic iron proceed at the maximum rates given by the kinetic theory of gases without any significant kinetic hindrances. On the other hand, evaporation of forsterite in vacuum and in

low-pressure hydrogen gas is kinetically more inhibited than metallic iron, and the evaporation coefficient ranges from 0.1 to 0.02 depending on temperature, hydrogen gas pressure, and crystallographic orientations. Anisotropic evaporation of forsterite leads to the change of shape of crystalline forsterite dust, which would result in the change of infrared spectral features and would be a powerful probe for dust-evolution in circumstellar environments.

Condensation experiments on forsterite have been carried out at low pressures in the system of Mg_2SiO_4-H_2-H_2O. Polycrystalline forsterite was obtained as condensates at 1160 K and the supersaturation ratio of 800-8000 and at 1275 K and the supersaturation ratio of 7-190. The condensation coefficient of forsterite has been estimated to be in the range of 0.09–0.006 although it should be refined in future studies. The smaller a_c of forsterite indicates less-efficient formation of forsterite dust than metallic iron in space.

Acknowledgements

References

[1] Ebel D. (2006) in Meteorites & the Early Solar System II, eds. D. S. Lauretta and H. Y. McSween Jr. (Tucson AZ: Univ. Arizona Press), 253.

[2] MacPherson G. J. (2005) in *Meteorites, Comets, and Planets (Treatise on Geochemistry 1),* ed. A. M. Davis (Elsevier), 201.

[3] Zinner E. K. (2005) in *Meteorites, Comets, and Planets (Treatise on Geochemistry 1),* ed. A. M. Davis (Elsevier), 17.

[4] Takigawa A. et al. (2014) *GCA,* 124, 309

[5] Gail H. -P. (2010) in *Astromineralogy,* ed. Th. Henning (Springer), 61.

[6] Brucato J. R. and Nuth J. A. III (2010) in *Protoplanetary Dust,* eds. D. Apai and D. S. Lauretta (Cambridge Univ. Press), 128.

[7] Tachibana S. et al. (2011) *ApJ,* 736, doi:10.1088/0004-637X/736/1/16.

[8] Takigawa A. et al. (2009) *ApJ,* 707, L97.

[9] Paule R. C. and Margrave J. L. (1967) in *The characterization of high-temperature vapors*, ed. J. L. Margrave (New York: Wiley), 130.

[10] Yamada M. et al. (2006) *Planet. Space Sci.,* 54, 1096.

[11] Ozawa K. et al. (2012) *Amer. Mineral.* 97, 80.

[12] Takigawa A. and Tachibana S. (2012) *ApJ,* 750, doi:10.1088/0004-637X/750/2/149